



---

Cell Lineage Analysis by Intracellular Injection of Fluorescent Tracers  
Author(s): David A. Weisblat, Saul L. Zackson, Seth S. Blair, Janis D. Young  
Source: *Science*, New Series, Vol. 209, No. 4464 (Sep. 26, 1980), pp. 1538-1541  
Published by: [American Association for the Advancement of Science](#)  
Stable URL: <http://www.jstor.org/stable/1684982>  
Accessed: 21/01/2011 19:51

---

Your use of the JSTOR archive indicates your acceptance of JSTOR's Terms and Conditions of Use, available at <http://www.jstor.org/page/info/about/policies/terms.jsp>. JSTOR's Terms and Conditions of Use provides, in part, that unless you have obtained prior permission, you may not download an entire issue of a journal or multiple copies of articles, and you may use content in the JSTOR archive only for your personal, non-commercial use.

Please contact the publisher regarding any further use of this work. Publisher contact information may be obtained at <http://www.jstor.org/action/showPublisher?publisherCode=aaas>.

Each copy of any part of a JSTOR transmission must contain the same copyright notice that appears on the screen or printed page of such transmission.

JSTOR is a not-for-profit service that helps scholars, researchers, and students discover, use, and build upon a wide range of content in a trusted digital archive. We use information technology and tools to increase productivity and facilitate new forms of scholarship. For more information about JSTOR, please contact [support@jstor.org](mailto:support@jstor.org).



*American Association for the Advancement of Science* is collaborating with JSTOR to digitize, preserve and extend access to *Science*.

<http://www.jstor.org>

they were killed. At this time, they weighed between 20 and 25 g. The mice were given a diet consisting of Purina laboratory chow and unlimited amounts of tap water. Both the food and water sources, the only sources of hydrogen, were characterized isotopically. Liver and muscle tissues from individual animals were dissected, frozen, dried, and analyzed.

A single species of snails and four species of algae were collected from three different tidal pools in Boothbay Harbor, Maine, by Drs. Wendy Harrison and Richard Wendlandt. The tidal pools were located at midtide level in a small harbor approximately 100 to 150 m from each other. The algal species were *Chondrus crispus* (Rhodophycophyta), *Fucus vesiculosus* (Phaeophycophyta), *Ulva lactuca* (Chlorophycophyta), and *Enteromorpha clathrata* (Chlorophycophyta). These algae were the dominant forms at this tidal level. The snails were of the species *Littorina obtusata* (5) and were collected attached to *Fucus* or browsing on the rocks beneath this algal species. Water samples were also collected from these pools and the Atlantic Ocean. The snails and the algae were kept frozen at  $-70^{\circ}\text{C}$  for 2 months. The snail tissue was then separated from the shell. After freeze-drying, the samples were placed in a vacuum oven at  $60^{\circ}\text{C}$  over  $\text{P}_2\text{O}_5$ .

Six to ten milligrams of the dried sample were combusted in a platinum boat at  $750^{\circ}\text{C}$  in an atmosphere of oxygen. The water from the combustion was trapped with liquid nitrogen, converted to  $\text{H}_2$ , and analyzed with an isotope-ratio mass spectrometer (Nuclide Corporation model RMS-3-60) (4). The results are reported in terms of  $\delta\text{D}$  (per mil), which is defined as

$$\delta\text{D} = \left[ \frac{(\text{D}/\text{H})_{\text{sample}}}{(\text{D}/\text{H})_{\text{standard}}} - 1 \right] 10^3$$

The hydrogen isotope standard was standard mean ocean water. This system for measuring hydrogen isotopes is routinely used on a variety of organic matter and typically yields results from triplicate analyses of these samples with a standard deviation of  $\pm 5$  per mil.

The hydrogen isotopic content of laboratory-reared mice (Fig. 1) is dependent on the isotopic content of their food source. The  $\delta\text{D}$  of mouse feces is related directly to that of the laboratory chow; the  $\delta\text{D}$  of urine is related to that of the available water. The small variation in  $\delta\text{D}$  among individuals, either mice or snails, corresponds with a similar variation in the  $\delta\text{D}$  of the food source and indicates that individual animals regulate

hydrogen metabolism to a similar extent as the whole population.

The results of the hydrogen isotope analyses for ten samples of *L. obtusata* and ten samples of algae of four different species are given in Fig. 1 and Table 1. The average  $\delta\text{D}$  for the snails from sites 1, 2, and 3 are the same, as indication that they have the same diet. Furthermore, 80 percent of the individual  $\delta\text{D}$  values are within  $\pm 5$  of the average. Of the four species of algae, only for *F. vesiculosus* does the  $\delta\text{D}$  show any obvious relation to the  $\delta\text{D}$  of the snails. The  $\delta\text{D}$  of *Fucus* ranges from  $-102$  to  $-116$ , or an average of  $-111$ , which compares with the  $\delta\text{D}$  of  $-111$  for the snails at the three sites.

A combination of *Chondrus* ( $\delta\text{D} = -92$ ) and *Ulva* ( $\delta\text{D} = -173$ ) in the snails' diet could account for the  $\delta\text{D}$  of the snails. *Littorina obtusata*, however, has been observed in nature and also in controlled laboratory experiments. Not only do these snails live and breed on *Fucus*, but they also consume *Fucus* as the primary dietary source (6).

The  $\delta\text{D}$  of the food source, not the water, determines for the most part the  $\delta\text{D}$  of the organically bonded hydrogen in animals. This observation is supported by the fact that the  $\delta\text{D}$  of the snails and their food source (*Fucus*) are similar in a

natural setting, even though the ambient water is more enriched in deuterium than the water in the laboratory study (7). Although there is greater variation in the  $\delta\text{D}$  of the diet and of the animal tissue than is seen in  $\delta^{13}\text{C}$  measurements, the relationship that "you are what you eat" applies to hydrogen isotopes. In these simple cases, the conclusion from hydrogen isotope measurements is in agreement with direct observation.

MARILYN F. ESTEP

HALINA DABROWSKI

*Geophysical Laboratory,  
Carnegie Institution of Washington,  
Washington, D.C. 20008*

#### References and Notes

1. M. DeNiro and S. Epstein, *Geochim. Cosmochim. Acta* **42**, 495 (1978); B. Fry, A. Joern, P. L. Parker, *Ecology* **59**, 498 (1978).
2. W. E. Sciegl and J. C. Vogel, *Earth Planet. Sci. Lett.* **7**, 307 (1970).
3. S. Epstein, C. J. Yapp, J. H. Hall, *ibid.* **30**, 241 (1976).
4. M. F. Estep and T. C. Hoering, *Geochim. Cosmochim. Acta*, in press.
5. J. Rosewater, personal communication.
6. J. J. Barkman, *Arch. Neerl. Zool.* **11**, 50 (1956); K. Bakker, *ibid.* **13**, 230 (1959).
7. The primary hydrogen isotope fractionation in living organisms occurs during photosynthesis in plants (4). The  $\delta\text{D}$  of algae that have been grown heterotrophically in the dark with either glucose or acetate is dependent on the  $\delta\text{D}$  of the organic food source rather than on the  $\delta\text{D}$  of the water.
8. We thank T. C. Hoering for invaluable assistance and discussions.

7 April 1980; revised 27 May 1980

## Cell Lineage Analysis by Intracellular Injection of Fluorescent Tracers

**Abstract.** *Cell lineages during development of the leech are revealed by injection of a fluorescent peptide, rhodamine-D-peptide, into identified embryonic cells. Use of this peptide together with a nuclear stain showed a stereotypic cleavage pattern of stem cells and their progeny. Combined injection of rhodamine-D-peptide and pronase demonstrated the arrest of stem cell production in the pronase-injected teloblast.*

We reported previously that injection of horseradish peroxidase (HRP) as a tracer enzyme into identified cells of early embryos makes possible the determination of cell lineages during embryonic development (1, 2). However, because the histochemical HRP reaction product is opaque, this method is unsuitable for experiments in which the mitotic state of tracer-labeled cells is to be examined in whole mount with nuclear staining. In addition, this method cannot be used to test the effectiveness of intracellular pronase injection as a means of ablating embryonic cells (3) because HRP is sensitive to proteolytic digestion. Fluorescent dye tracers would overcome both these limitations, but such small

molecules (molecular weight on the order of 500) cannot be used directly as cell lineage tracers because upon injection they diffuse throughout the entire embryo (1), presumably via intercellular gap junctions (4). A fluorescent dye could be confined to the injected cell and its lineal descendants if attached to a larger carrier molecule, since it has been reported that the molecular weight limit for the permeation of insect salivary gland gap junctions by oligopeptide-fluorescent dye complexes is between 1200 and 1900 (4). To be suitable for cell lineage tracing, the carrier molecule should be of an appropriate size, have chemical sites to which the dye can be coupled, be reactive with histological fixatives, and

resist the action of proteolytic enzymes. We found that the dodecapeptide (Glu-Ala)<sub>2</sub>-Lys-Ala-(Glu-Ala)<sub>2</sub>-Lys-Gly (5), which has a molecular weight of about 1200 and is composed of amino acids in the unnatural D-configuration, meets these requirements. We synthesized this peptide by the Merrifield solid phase method (6). The synthetic peptide was coupled to rhodamine isothiocyanate, and the product, rhodamine-D-peptide (RDP), was isolated by column chromatography and lyophilized (7). In a similar manner, a fluorescein derivative of the peptide (FDP) was prepared.

The utility of RDP as a cell lineage tracer was demonstrated in experiments with embryos of the glossiphoniid leech *Helobdella triserialis*, whose initial development has been divided into eight stages (2). Beginning with the uncleaved egg (stage 1), the *Helobdella* embryo undergoes a series of stereotyped cleavages that result (by stage 6c) in one bilateral pair of mesodermal precursor cells, the M teloblasts, and four bilateral pairs of ectodermal precursor cells, the N, O, P, and Q teloblasts (Fig. 1a). Individual teloblasts can be identified by their size and position within the embryo. Each teloblast undergoes a series of unequal cleavages to produce a column, or bandlet, of smaller stem cells (designated by the lower case letter corresponding to the parent teloblast). The five stem cell bandlets on each side join to form a pair of germinal bands (early in stage 7). Within each germinal band the ectodermal bandlets lie superficially, with the n bandlet most lateral and the q bandlet most medial; the mesodermal, or m bandlet, lies underneath. Right and left germinal bands meet at the future head (early in stage 8) (Fig. 1b) and then coalesce, zipper-like, along the future ventral midline to form the germinal plate. As a result of this coalescence (which is complete at the end of stage 8), the n bandlets become most medial and the q bandlets most lateral in the germinal plate. Segmental structures, such as the ventral nerve cord ganglia, arise by proliferation of germinal plate cells. This development of the segmental structures occurs in a rostro-caudal sequence, so that the more anterior the position of a segment in the germinal band or germinal plate, the further its development has progressed.

In order to study the cell cleavage pattern within the germinal bandlets, a teloblast (or teloblast precursor) was injected with RDP. After formation of the germinal bands was under way (that is, at stage 7 or 8), the embryo was fixed and

treated with the blue-fluorescing, DNA-specific stain Hoechst 33258 (8). The blue fluorescence of the nuclei and the red fluorescence of the RDP-labeled cytoplasm were then viewed separately through appropriate filters. By focusing through the cleared embryo, we could trace the red-fluorescing bandlet from its point of origin at the teloblast to its final position in the germinal band. Figure 2a shows an embryo whose left N teloblast had been injected with RDP at stage 6a. The embryo was fixed and stained with Hoechst 33258 at early stage 8. The numerous blue dots visible in this photograph represent nuclei of diverse embryonic cells, but the nuclei belonging to the n bandlet can be distinguished because they lie within red (that is, RDP-labeled) N teloblast progeny. Closer inspection of bandlet nuclei showed that they are of two types: interphase nuclei with diffuse fluorescence and mitotic nuclei with brightly fluorescent, condensed chromosomes (8) (Fig. 2b). The alignment of condensed chromosomes on the metaphase plate indicates the orientation of

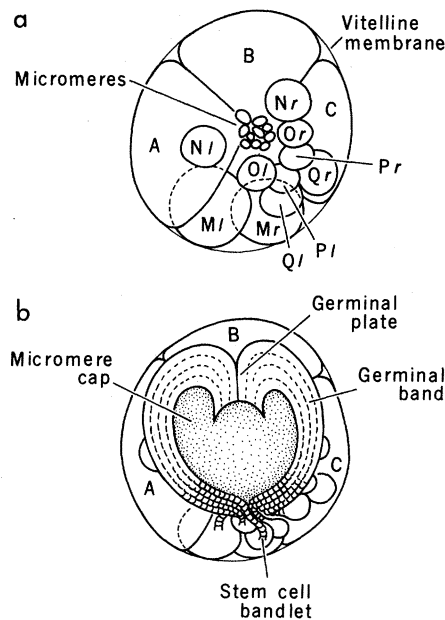


Fig. 1. Schematic representation of two early developmental stages of the leech *Helobdella triserialis*. (a) Stage 6c. Stereotyped cleavages have resulted in the formation of three large blastomeres A, B, and C; five pairs of teloblasts, Ml and Mr, Nl and Nr, Ol and Or, Pl and Pr, and Ql and Qr; as well as a group of small cells, the micromeres. (b) Early stage 8. Each teloblast has formed a stem cell bandlet. The five bandlets on each side have joined to form the left and right germinal bands. The germinal bands have grown over the surface of the three large blastomeres, joined at the future head, and begun rostro-caudal coalescence along the ventral midline. Proliferation of micromeres has given rise to the micromere cap. The diameter of the embryo is about 500  $\mu\text{m}$ .

the spindle axis of cell division. Upon examination of 26 stage 7 embryos in which an N teloblast had been injected with RDP at stage 6, we found no mitotic n stem cells at a separation of less than 20 stem cells from the parent teloblast. (At that point the bandlet cells are already within the germinal band.) The spindle axes of all observed early n stem cell divisions were nearly parallel to the long axis of the bandlet (Fig. 2b). After that first division, therefore, the bandlet still remains one cell wide. Figure 2c shows a similarly treated embryo whose M teloblasts had been labeled with RDP by injecting their precursor, cell DM, at stage 4b. In this figure, progeny of m bandlet stem cell mitoses are visible at a distance of about ten cells from the M teloblast, before that bandlet had joined the ectodermal n, o, p, and q bandlets in the germinal band. The spindle axis of the initial stem cell division in the m bandlet is perpendicular to the long axis of the bandlet, so that the m bandlet becomes two cells wide after the first stem cell division. Similar observations were made in 17 RDP-labeled m bandlets. Thus, combined use of RDP and Hoechst 33258 reveals that the mesodermal m stem cells differ from the ectodermal n stem cells in both the timing and the orientation of their first cleavage—whereas the n stem cells cleave only after entering the germinal band, with spindle axes parallel to the long axis of the bandlet, the m stem cells cleave prior to entering the germinal band, with spindle axes perpendicular to the long axis of the bandlet.

Figure 2d presents an embryo in which the left M teloblast had been injected with RDP at stage 5. In the most rostral sector of the labeled (left) germinal band, segmentation of the mesodermal tissue can be observed, even before its fusion with the right germinal band. Stem cells of the left m bandlet labeled with RDP have given rise to clusters of RDP-labeled progeny. The arrangement of the progeny is similar in adjacent clusters (see Fig. 2e). This similarity suggests that the early development of the mesoderm of each body segment proceeds, as does teloblast formation, by stereotyped cell divisions.

Injection of RDP has also been used in conjunction with cell ablation by pronase injection (9) in *Helobdella* embryos. As was shown by the HRP tracer method, a topographically coherent fraction of the neurons on one side of each segmental ganglion is derived from the ipsilateral N teloblast (1, 2). Furthermore, injecting pronase into an N teloblast pri-



or to completion of its stem cell production results in abnormal development of the ipsilateral half of the segmental ganglia (3). The teloblast may be killed outright by pronase injection, with complete arrest of stem cell production; but it is

also possible that the teloblast is merely damaged and continues to produce stem cells in an abnormal manner. In order to ascertain whether the morphological abnormalities following pronase injection are due to a disturbance of stem cell pro-

duction or to its complete arrest, it is necessary to identify the progeny, if any, of the injected teloblast. Horseradish peroxidase cannot be used for this purpose because it is sensitive to proteolytic digestion. Therefore, the following ex-

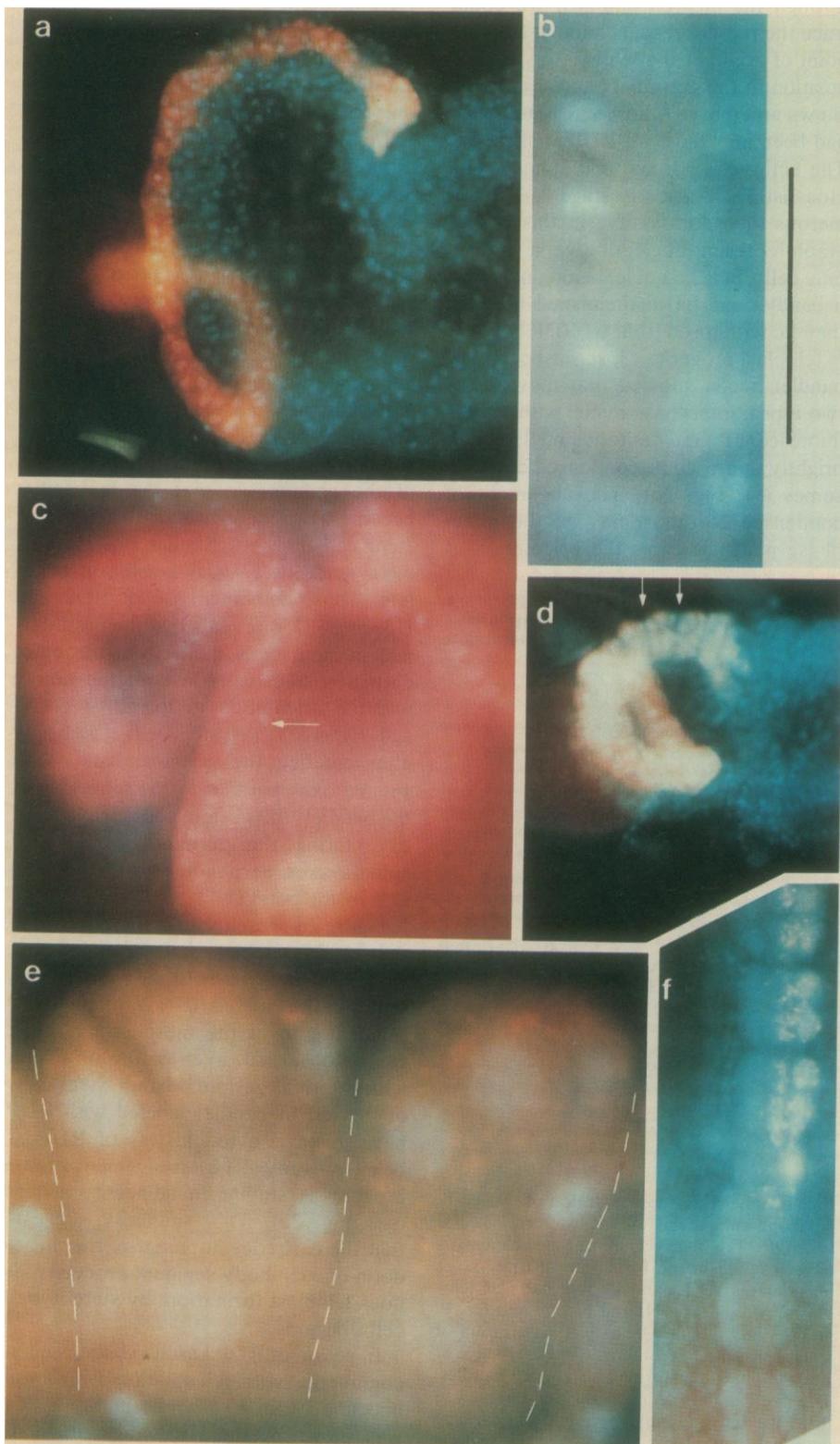


Fig. 2. Photomicrographs of *Helobdella* embryos injected with RDP and stained with Hoechst 33258. (a) Early stage 8 embryo (see Fig. 1b) whose cell *Nl* had been injected with RDP at stage 6a. The red *n* bandlet extends caudally from its origin at the *N* teloblast (left) to its point of entry into the left germinal band (bottom), then rostrally along the lateral edge of the germinal band to the future head (top right). The numerous blue dots are nuclei of cells of the germinal bands and micromere cap. (b) Enlarged view of the *n* bandlet of an embryo treated in the same way as the one shown in (a). In the middle of this picture is a telophase cell with the axis of division parallel to the longitudinal axis of the bandlet. Above and below the dividing cell, interphase nuclei are visible. (c) Early stage 8 embryo whose *M* teloblast precursor, cell *DM*, had been injected with RDP at stage 4b. The left *m* bandlet extends from the left *M* teloblast (out of focus at bottom center) to the point of origin of the germinal band (in focus at top center). Part of the right *m* bandlet can be seen in the upper right-hand portion. Interphase nuclei are visible as pale dots within the *m* bandlet. The arrow points to the daughter cells of an *m* stem cell cleavage that took place prior to the entry of the bandlet into the germinal band. The position of the daughter cell nuclei indicates that the axis of division was perpendicular to the longitudinal axis of the bandlet. Rows of nuclei of unlabeled ectodermal bandlets converge at the point of origin of the germinal band. (d) Late stage 7 embryo whose cell *Ml* had been injected with RDP at stage 5. The red *m* bandlet extends from its origin at the *M* teloblast (left) to its point of entry into the germinal band (center), then in an arc beneath the ectodermal bandlet to the future head (top center). The arrows indicate two adjacent clusters of *m* stem cell progeny. (e) Enlarged view of the cell clusters marked by arrows in (d) showing some of the cells in each cluster. Borders between adjacent clusters are marked by broken lines. Topographically and morphologically corresponding cells can be seen within these clusters. (f) Ventral view of a portion of the nerve cord of a 9-day-old embryo whose cell *Nl* had been injected with RDP at stage 6a and with pronase at stage 7. Anterior is at the top; seven ganglia are shown. Ganglia 1, 2, and 3 (from the top) are normal; RDP-labeled cells can be seen in the left (apparent right) sides of these ganglia. Ganglia 6 and 7 are abnormal, in that they contain fewer cells on the left (apparent right) side; the remaining cells are not labeled with RDP. Ganglion 4 (tilted and only partially visible) and ganglion 5 are at the border between the normal anterior and the abnormal posterior parts of the nerve cord; ganglion 4 contains some RDP-labeled cells at its left lateral edge, and ganglion 5 at its left anterior midline. The red background beneath ganglia 6 and 7 results from the fluorescence of RDP

and of the dye Fast Green [coinjecting with pronase (9)] in teloblast remnants in the gut. All the embryos shown in this figure were fixed and acid-cleared by the method of Fernandez (10), except that the fixative included 2.5  $\mu\text{g}$  of Hoechst 33258 per milliliter of fixative. After fixation (12 to 24 hours at 4°C) the embryos were mounted between cover slips in 75 percent glycerol containing 2.5  $\mu\text{g}$  of Hoechst 33258 per milliliter. Double-exposure photomicrographs were made under epi-illumination from either a 75W tungsten-halogen or 50W mercury light source, first through Zeiss filter set 48 77 14 and then through Zeiss filter set 48 17 02. Scale bar, 160  $\mu\text{m}$  in (a), (c), and (f); 25  $\mu\text{m}$  in (b) and (e); and 250  $\mu\text{m}$  in (d).

periment was carried out with RDP, which is pronase-resistant.

At stage 6a, prior to the onset of n bandlet stem cell production, an N teloblast was injected with RDP. At stage 7, after stem cell production was under way, the same N teloblast was reinjected with pronase; Fig. 2f shows such an embryo at 9 days of age. The anterior part of the nerve cord of this embryo consists of morphologically normal (bilaterally symmetric) ganglia, whereas the posterior part consists of abnormal (bilaterally asymmetric) ganglia deficient in cell number on the side of the ablated N teloblast. Moreover, anterior ganglia contain neurons labeled with RDP, whereas posterior ganglia do not. The boundary between anterior morphologically normal and posterior morphologically deficient ganglia coincides with the boundary between anterior RDP-labeled and posterior unlabeled ganglia. Thus it follows that the anterior ganglia of the pronase-treated embryo contain progeny of n stem cells produced prior to ablation of the N teloblast and that the posterior ganglia are abnormal because they received no cellular contribution from the N teloblast.

The fluorescent peptides RDP and FDP have further advantages as cell lineage tracers: (i) The red-fluorescing RDP and the yellow-fluorescing FDP can be used in combination for double-label experiments; and (ii) their distribution can be observed in living embryos, in contrast to that of HRP, which can be visualized only in fixed preparations. Thus these fluorescent tracers should make it possible to follow the appearance of successive descendants of an injected early embryonic cell in the same preparation and to know the embryonic origin of nerve and muscle cells identified by intracellular electrophysiological recordings.

DAVID A. WEISBLAT  
SAUL L. ZACKSON  
SETH S. BLAIR  
JANIS D. YOUNG\*

Department of Molecular Biology,  
University of California, Berkeley 94720

#### References and Notes

1. D. A. Weisblat, R. T. Sawyer, G. S. Stent, *Science* **202**, 1295 (1978).
2. D. A. Weisblat, G. Harper, G. S. Stent, R. T. Sawyer, *Dev. Biol.* **76**, 58 (1980).
3. D. A. Weisblat, S. Blair, G. S. Stent, *Soc. Neurosci. Abstr.* **5**, 184 (1979).
4. I. Simpson, B. Rose, W. R. Loewenstein, *Science* **195**, 294 (1977).
5. Abbreviations: Ala, alanine; Glu, glutamate; Gly, glycine; and Lys, lysine.
6. J. M. Stewart and J. D. Young, *Solid Phase Peptide Synthesis* (Freeman, San Francisco, 1969). Each coupling step proceeded to greater than 99 percent completion, as judged by the ninhydrin test. The composition of the synthetic peptide was confirmed by amino acid analysis of an acid hydrolyzate.

7. R. C. Nairn, *Fluorescent Protein Tracing* (Williams and Wilkins, Baltimore, 1969). Forty milligrams (30  $\mu$ mole) of the peptide triacetate were added to 0.24 ml of 1N NaOH and then suspended in 2 ml of 0.5M carbonate-bicarbonate buffer, pH 9.0. Thirty-two milligrams (60  $\mu$ mole) of rhodamine-B isothiocyanate (Sigma; mixed isomers, molecular weight 536) were dissolved in 4 ml of acetone (some material failed to dissolve) and added drop by drop to the peptide suspension with constant stirring at room temperature. After several hours the reaction mixture was filtered, and the filtrate was passed over a Sephadex G-25 column in 0.05M ammonium acetate. Dye-containing fractions were identified by their color, pooled, and lyophilized. A fast-running, weakly fluorescent fraction emerged from the column ahead of the peptide fraction; whether this material represents an impurity in the dye or a side product of the labeling procedure was not determined. The average molar dye/peptide ratio was not measured but is

presumably less than 2; since the amino group of the  $\text{NH}_2$ -terminal glutamic acid residue ( $pK \sim 9.5$ ) is apt to react faster than the epsilon amino group of the lysine residues ( $pK \sim 10.8$ ), we assume that essentially every RDP molecule has one or more free amino groups available for reaction with aldehyde fixative.

8. J. Sedat and L. Manuelides, *Cold Spring Harbor Symp. Quant. Biol.* **42**, 331 (1977).
9. I. Parnas and D. Bowling, *Nature (London)* **270**, 626 (1977).
10. J. Fernandez, *Dev. Biol.* **76**, 245 (1980).
11. We thank W. W. Stewart, J. W. Sedat, and G. S. Stent for helpful suggestions and discussions. Supported by NIH research grants NS 12548 and NS 12818 and NSF research grant BNS77-19181.

\* Present address: Ralph Lowell Laboratories, McLean Hospital, Belmont, Massachusetts 02178.

31 December 1979; revised 22 February 1980

## *Naegleria fowleri*: Trimethoprim Sensitivity

**Abstract.** *Trimethoprim in a concentration of 4 micrograms per milliliter of Bacto-Casitone (Difco) medium inhibits the growth of nonvirulent Naegleria fowleri isolates. The growth of virulent strains is unaffected even with 400 micrograms of the drug per milliliter of medium. Differences in sensitivity constitute the possibility of a simple selection of environmental isolates. The pathogenicity and virulence of Naegleria species may be connected with the metabolism of folic acid.*

In an attempt to find simple markers by which we could differentiate among the various species, strains, or variants of amoebas of the genus *Naegleria* we tested—among other factors—the effect of several chemotherapeutics on the growth of *Naegleria fowleri* in axenic cultures. We observed that some strains were inhibited under defined conditions by low concentrations of trimethoprim [2,4-diamino-5-(3,4,5-trimethoxybenzyl)pyrimidine].

We used a total of 31 strains of *N. fowleri* in the experiments. Ten of them were isolated from human cases of primary amoebic meningoencephalitis and 21 strains were isolated from water samples of warm industrial effluents in Czechoslovakia. Three of these environmental strains were pathogenic for laboratory animals. The basic tests were carried out in tubes containing 5 ml of fluid BCS medium, that is, 2 percent Bacto-Casitone (Difco) in distilled water with 10 percent of fresh rabbit serum (1). Trimethoprim (2) was added to this medium in concentrations ranging from 0.4  $\mu$ g/ml to 400  $\mu$ g/ml. The tubes inoculated with the different strains of amoebas were incubated at 37°C.

All the nonvirulent isolates of *N. fowleri* were completely inhibited by trimethoprim in concentrations of 4  $\mu$ g/ml and higher. The strains isolated from humans and the virulent strains from the industrial effluents tolerated the highest tested concentrations of the drug without any definite changes of growth rate. Several other antagonists of folic acid such as aminopterin, 3,5-diaminopterin, and

methotrexate (3) applied in concentrations up to 50  $\mu$ g/ml under identical experimental conditions did not affect the growth of any of the *N. fowleri* strains.

The inhibitory effect of trimethoprim on nonvirulent environmental strains could be prevented by addition of folic acid or leucovorin (3) to the medium in concentrations of 50  $\mu$ g/ml. However, 2-amino-4-hydroxy-6-(tetrahydroxybutyl)pteridin (3) had no antagonistic effect on trimethoprim. Culture media containing such ingredients as liver digests or extracts; yeast extracts, peptones, or a suspension of thermally killed bacteria are inconvenient for experiments with trimethoprim activity because of their folic acid content.

The effect of trimethoprim on *N. fowleri* in BCS medium provides a simple and reliable method for differentiation of virulent and nonvirulent strains of this organism isolated in ecological and epidemiological environmental studies. Further examination of the differences in the metabolism of folic acid in *N. fowleri* may help to elucidate the conditions of pathogenicity and virulence of *Naegleria* species.

LUBOR ČERVA

Czechoslovak Academy of Sciences,  
Institute of Parasitology,  
Prague, Czechoslovakia

#### References and Notes

1. L. Červa, *Science* **163**, 576 (1969).
2. Obtained from Burroughs Wellcome and Co., London.
3. Obtained from K. Slavík, Laboratory of Protein Metabolism, Faculty of General Medicine, Charles University, Prague.

28 March 1980